

Effect of hydrostatic pressure on ferromagnetism in two-dimensional CrI₃

Suchanda Mondal¹, Murugesan Kannan², Moumita Das¹, Linganani Govindaraj²,
Ratnadwip Singha¹, Biswarup Satpati¹, Sonachalam Arumugam² and Prabhat Mandal¹
¹*Saha Institute of Nuclear Physics, HBNI, 1/AF Bidhannagar, Calcutta 700 064, India and*
²*Centre for High Pressure Research, School of Physics,*
Bharathidasan University, Tiruchirappalli 620 024, India
(Dated: April 30, 2022)

We have investigated the magnetic properties of highly anisotropic layered ferromagnetic semiconductor CrI₃ in presence of hydrostatic pressure (P). At ambient pressure, magnetization exhibits a clear anomaly below 212 K along with a thermal hysteresis over a wide temperature range (212-180 K), where a first-order structural transition is observed. CrI₃ undergoes a second-order ferromagnetic-paramagnetic phase transition with Curie temperature $T_C=60.4$ K. With application of pressure, the transition becomes sharper and T_C is found to increase from 60.4 to 64.9 K as P increases from 0 to 1.0 GPa. T_C increases with P in a sublinear fashion. The thermal hysteresis in magnetization and the increase of T_C with pressure suggest that the spin and lattice degrees of freedom are coupled. The observed increase in T_C has been explained on the basis of change in inter-layer coupling and Cr-I-Cr bond angle with pressure.

Two-dimensional ferromagnetic (FM) semiconductors exhibit a wide range of novel electronic properties with immense potential for application in different magnetoelectronic technology.[1–4] In spintronic devices, electron spin, instead of or in addition to charge degrees of freedom, is used for information storage and processing.[5–9] This can be realized, when magnetism is incorporated into the active materials. Low-dimensional magnetic systems with intrinsic ferromagnetism have also received considerable interest for fundamental research due to the occurrence of several quantum phenomena.[10–15] Layered FM semiconductors are very rare in nature due to the absence of long-range magnetic ordering. According to the Mermin-Wagner theorem, two-dimensional isotropic Heisenberg model does not show long-range magnetic ordering at any finite temperature.[11] Recently, two different types of layered FM semiconductors with weak inter-layer van der Waals interaction namely chromium trihalides, CrX₃ ($X = \text{Cl, Br, I}$), and chromium-based ternary compounds, Cr₂X₂Te₆ ($X = \text{Si, Ge}$), have received considerable attention as promising candidates for both fundamental research and possible application in spintronics technology owing to their long-range ferromagnetism in bilayer or monolayer and easy exfoliation property.[16–23] Among the different members of Cr₂X₂Te₆ and CrX₃ series, bulk Cr₂Ge₂Te₆ and CrI₃ compounds exhibit highest FM transition temperatures (T_C) 68 and 61 K, respectively. Though, their T_C s are comparable, in contrast to Cr₂Ge₂Te₆, magnetic interaction is much more anisotropic in CrI₃ due to the very weak coupling between the layers and ferromagnetism retains down to single layer, with transition temperature as high as 45 K, whereas bilayer CrI₃ is antiferromagnetic. [18] Also, an extremely high tunneling magnetoresistance (10⁵ %) has been achieved in an exfoliated thin film of CrI₃. [21]

Unlike chemical substitution, hydrostatic pressure (P) is a continuously tunable thermodynamic parameter

which can be used to tune the phase transition as well as charge conduction mechanism without introducing disorder in the system. Pressure primarily alters the bond lengths and bond angles of crystal lattice which, in turn, affect the inter-site electron hopping process. As a result, both transport and magnetic properties may change significantly with application of pressure. For example, several systems undergo pressure-induced insulator to metal transition.[24–26] Even, exotic phenomenon like superconductivity close to room temperature can be achieved by applying high pressure.[27] In perovskite manganites, both electronic and magnetic subsystems are found to be highly susceptible to external pressure as well as chemical pressure arising due to the variation of ionic size.[28–30] However, the role of pressure on T_C in insulating FM is very complicated and debatable due to the competition between direct exchange and superexchange. It is believed that as a result of compression, the superexchange interaction strength increases and the pressure coefficient of T_C is proportional to isothermal compressibility.[31] Though, T_C is observed to increase with P in several insulating FM, there are examples where T_C decreases with P . [31] Very recently, the effect of pressure on structural and magnetic properties has been investigated for two-dimensional ferromagnet Cr₂Ge₂Te₆. [32] It has been observed that T_C decreases monotonically with pressure up to 1 GPa. Also, a small but negative pressure coefficient of T_C has been reported for CrBr₃. [33] On the other hand, T_C is found to increase in layered VI₃ above a critical value of applied pressure.[34] So, it is important to investigate systematically the role of pressure on ferromagnetism in several insulating layered FM. In the present work, we have studied the effect of hydrostatic pressure on magnetic properties of well characterized single crystalline sample of CrI₃. In contrast to Cr₂Ge₂Te₆ and CrBr₃, T_C in CrI₃ is observed to increase monotonically with pressure. Also, the width of transition becomes sharper with pressure. This difference in the dependence

of T_C on P in these systems can be attributed to their crystallographic structure and the nature of bondings.

High quality plate-like single crystals of CrI_3 were grown by standard chemical vapor transport technique from an intimate mixture of high purity elements. Very fine granules of chromium (99.995%, Alfa Aesar) and anhydrous iodine globules (99.99%, Alfa Aesar) were mixed in a molar ratio 1:3 in argon atmosphere. The well-mixed powder was sealed in an evacuated quartz tube and placed inside a gradient furnace for a period of 7 days. The one end of the tube containing the powder was maintained at 650°C , while the other end was kept at 600°C . Single crystals of few mm in size were formed at the cold end of the tube, which were extracted mechanically and characterized. The crystals were freshly cleaved before characterizations and measurements. Phase purity and the structural analysis of the samples were done in a high-resolution x-ray diffractometer (Rigaku, TTRAX III), using $\text{Cu-K}\alpha$ radiation and high-resolution transmission electron microscopy (HRTEM) in an FEI, TECNAI G^2 F30, S-TWIN microscope operating at 300 kV and equipped with a GATAN Orius SC1000B CCD camera. The elemental composition was checked by energy-dispersive x-ray spectroscopy (EDX) using the same microscope with a scanning unit and a high-angle annular dark-field scanning (HAADF) detector from Fischione (Model 3000). The magnetic measurements at ambient pressure were done in a 7 T SQUID-VSM (MPMS3, Quantum Design). The dc magnetization measurements under pressure were done using physical property measurement system (Quantum Design). The external pressure up to 1 GPa was generated by a clamp type miniature hydrostatic pressure cell which is made of nonmagnetic CuBe alloy. The fluorinert FC 70 and FC 77 mixture (1:1) was used as a pressure transmitting medium and the in-situ pressure was estimated from the superconducting transition of pure Sn.

The x-ray diffraction was performed on a cleaved thin single crystal of CrI_3 with flat surface. As shown in Fig. 1(a), the presence of very sharp $(0\ 0\ l)$ peaks in the diffraction pattern confirms that the flat plane of the crystal is perpendicular to the crystallographic c -axis with interlayer separation $6.658\ \text{\AA}$ and the peak positions correspond to $c=7.008\ \text{\AA}$, which is consistent with earlier reports.[16, 19] The crystal structure of CrI_3 is shown in Fig. 1(b). CrI_3 crystallizes in monoclinic AlCl_3 structure with $C2/m$ space group symmetry and undergoes a structural phase transition at around $T_S\sim 210\text{-}220\ \text{K}$ to rhombohedral BiI_3 structure with $R3$ symmetry.[16] In CrI_3 , the Cr^{3+} ions are in high spin state with the magnetic moment oriented in the out of plane direction and form a honeycomb network like a single layer of graphene, where each Cr^{3+} ion is surrounded by an edge-sharing octahedron of six iodine ions. In Fig. 2(a), we have shown the HRTEM image of

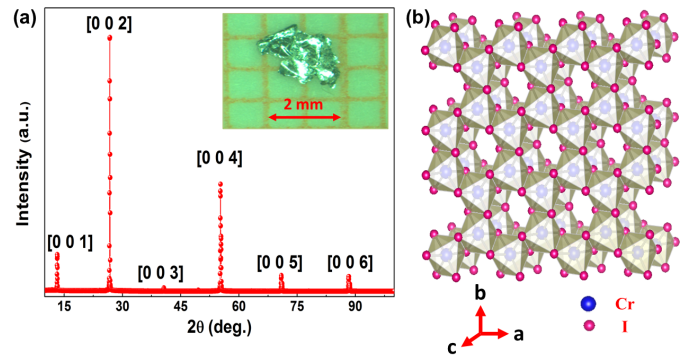


FIG. 1. (Color online) (a) X-ray diffraction pattern obtained from the cleaved plane of a CrI_3 crystal at room temperature. The picture of a typical platelike single crystal is shown in the inset. (b) The monoclinic crystal structure of CrI_3 viewed along the crystallographic ab -plane.

a typical single crystal, which reveals the high crystalline quality of the samples over a macroscopic length scale. From the interlayer separation as shown in figure, we have calculated the value of the lattice parameter $a=6.8\ \text{\AA}$, which is also close that reported from powder x-ray diffraction. [16, 19] Figure 2(b) illustrates the selected area electron diffraction pattern created by the crystallographic planes. The obtained results from the EDX spectroscopy at different randomly selected regions of the grown crystals confirm the homogeneous distribution of the elements and the chemical composition of the crystal is very close to the starting stoichiometry $\text{Cr:I}=1:3$ [Fig. 2(c)]. In Fig. 2(d), we have shown the EDX spectrum obtained on one such small area, as a representative.

The temperature dependence of dc magnetization (M) for the bulk single crystal of CrI_3 has been measured both under zero-field-cooled (ZFC) and field-cooled (FC) conditions in the temperature range 2-350 K. Figures 3(a) and (b) display $M(T)$ curves at 500 Oe with field parallel to the c axis and ab plane, respectively. In the paramagnetic (PM) state, M in the FC and ZFC cycles does not split from each other and increases monotonically with decreasing temperature. At around 61 K, M shows an abrupt increase, an indication of long-range ferromagnetic ordering at $T_C\sim 60.4\ \text{K}$, determined from the position of the minimum in the dM/dT versus T curve. T_C determined from $dM(T)/dT$ curve is very close to that reported from the critical behavior analysis of magnetization data.[19] In the FM state, a small hysteresis is observed between FC and ZFC magnetization. At low applied field, a weak kink-like anomaly is seen slightly below T_C , which is more prominent for field parallel to ab plane. This anomaly in M has been characterized as a two-step magnetization but the exact origin of such behavior is yet to decipher.[35] It is well known that on cooling, CrI_3

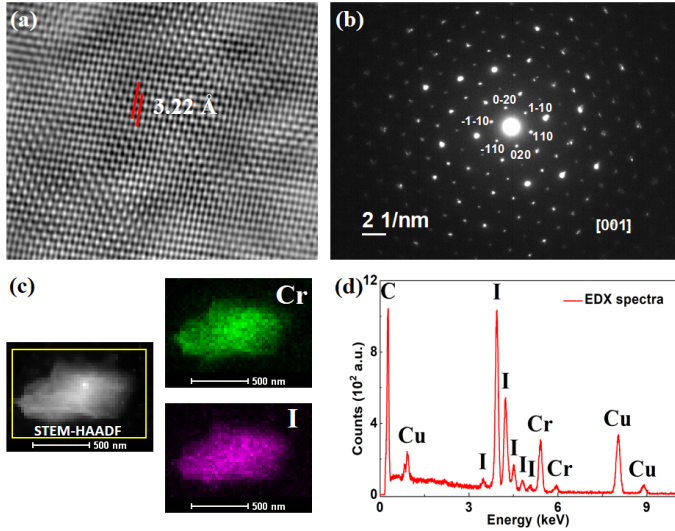


FIG. 2. (Color online) (a) High-resolution transmission electron microscopy (HRTEM) image of the CrI_3 single crystal. (b) Selected area electron diffraction pattern obtained from a single grain. (c) Elemental mapping of a randomly selected grain showing the homogeneity of the elements in the sample. (d) A typical energy-dispersive x-ray (EDX) spectrum of the CrI_3 crystal. The characteristic copper and carbon peaks in the spectrum are coming from the carbon coated copper grid, on which the samples were mounted for TEM measurements.

exhibits a temperature-induced crystallographic phase transition from monoclinic to rhombohedral structure below T_S . The high-temperature monoclinic and the low-temperature rhombohedral phases coexist over a wide range of T and the structural parameter (c -axis) shows a strong thermal hysteresis. [16] The coexistence of two phases along with thermal hysteresis between cooling and warming cycles suggest that the phase transition is first-order in nature. In order to know whether this structural transition can be observed in magnetic properties, magnetization has been measured by cooling the sample from room temperature down to 2 K in presence of field and upon subsequent warming at different applied fields up to 7 T, as shown in Figs. 3(c) and (d). It is clear from the $M(T)$ curves that M displays an anomaly around the structural transition T_S and the cooling and heating cycle data do not overlap each other but display a significant thermal hysteresis over a wide temperature range 212-180 K, which is consistent with the reported temperature dependent x-ray diffraction. [16] Though the value of magnetization changes with field strength, the nature of T dependence of M is insensitive to applied magnetic field. We have also done magnetization measurements with field parallel to ab plane. Qualitative similar behavior has been observed. For further understanding of the nature of the magnetic interaction, the temperature dependence of inverse susceptibility χ^{-1} of CrI_3 has been analysed [Fig. S1 in supplementary information]. [36] A linear fit to χ^{-1} data above T_S reveals the Curie-Weiss temperature $\theta_{CW}=77$

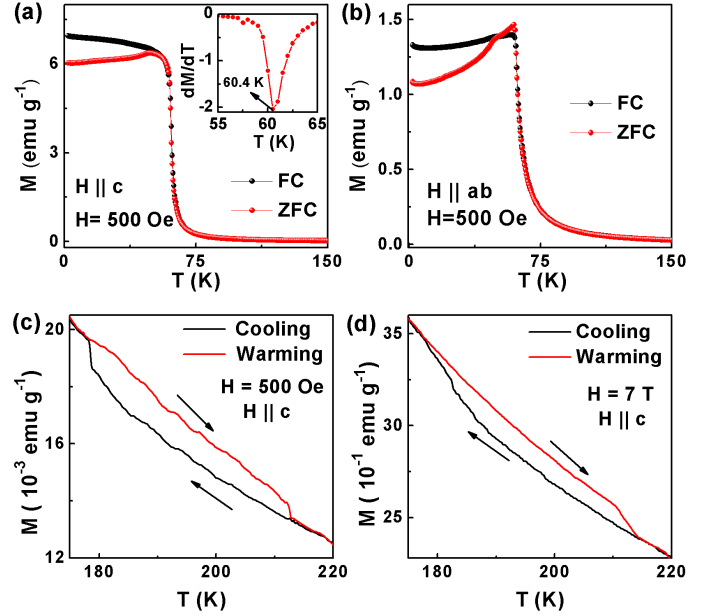


FIG. 3. (Color online) Temperature dependence of zero-field-cooled and field-cooled magnetization for CrI_3 measured with magnetic field applied along the (a) c -axis and parallel to the (b) ab -plane. The inset shows dM/dT as a function of T and Curie temperature (T_C). Field-cooled magnetization for heating and cooling cycles with magnetic field (c) 500 Oe and (d) 7 T, applied along c -axis. A clear anomaly along with thermal hysteresis can be seen around the structural transitional region (below ~ 212 K).

K and the effective moment $\mu_{eff} = 3.77 \mu_B/\text{Cr}$ which is close to the theoretical value ($3.87 \mu_B$) expected for Cr^{3+} in the high-spin state. Isothermal magnetization has also been measured at different temperatures [Fig. S2 in supplementary information]. [36] Well below the T_C , $M(H)$ curves show saturation behavior at high fields and the value of saturation magnetic moment at 2 K and 5 T is $2.98 \mu_B/\text{Cr}$ ion.

To capture the salient features of ferromagnetism under pressure, FC magnetization data have been plotted as a function of temperature for different applied pressures as shown in Fig. 4(a). It is clear from the figure that with increase in pressure, the value of M decreases and the transition region shifts slowly toward higher temperature side, indicating that pressure stabilises the ferromagnetic state. For the $\text{Cr}_2\text{Ge}_2\text{Te}_6$ system, initially M increases with pressure and then decreases slowly and M is slightly smaller at ambient pressure. In order to determine the actual dependence of T_C on pressure, T_C has been estimated from the dM/dT versus T curves as in the case of ambient pressure. For each pressure, dM/dT curve shown in the inset of Fig. 4(a), exhibits a very sharp minimum and its position shifts progressively toward higher temperature side with increasing pressure. Thus, the FM-PM transition in

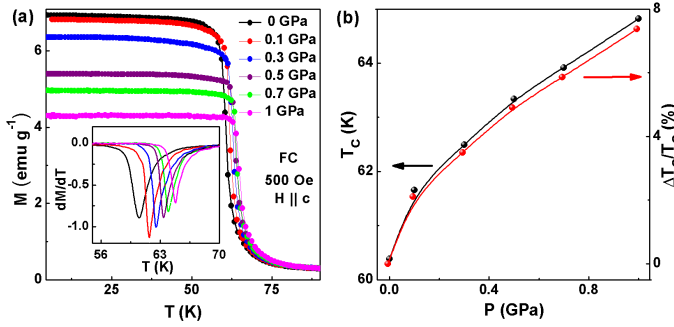


FIG. 4. (Color online) (a) Temperature dependence of field-cooled magnetization for CrI_3 at different applied pressures with magnetic field applied parallel to the c -axis. Inset shows dM/dT as a function of T for different pressures. (b) T_C , determined from the position of the minimum of dM/dT curves, plotted as a function of pressure along with the relative change in T_C ($\Delta T_C/T_C$).

CrI_3 remains very sharp with the application of pressure up to 1 GPa. Indeed, we observe that the full-width at half-minimum of dM/dT vs. T curve is smaller for $P > 0$. In particular, the transition is very sharp for $P = 0.1$ GPa. For $\text{Cr}_2\text{Ge}_2\text{Te}_6$ the transition becomes broad in presence of pressure. The pressure variation of T_C has been demonstrated in Fig. 4(b). This figure shows that the dependence of T_C on pressure is not linear but $T_C(P)$ curve exhibits a weak downward curvature. Initially, T_C increases very rapidly with pressure at the rate of ~ 12 K/GPa up to about 0.10 GPa and then increases slowly. For $P \geq 0.5$ GPa, T_C increases approximately linearly with a pressure coefficient, $dT_C/dP \sim 3$ K/GPa. To illustrate the effect of pressure on FM transition, we have also calculated the relative change in T_C , defined as $\Delta T_C/T_C = [T_C(P) - T_C(0)]/T_C(0)$, which has been plotted along with T_C . This plot shows that T_C increases by about 7.5 % for applied pressure of 1 GPa. Though M in the FM state decreases systematically with the increase in pressure, $M(H)$ curve at 2 K shows saturation-like behavior above 2 T with saturation magnetic moment close that observed at ambient pressure. This suggests that the Cr^{3+} remains in the high-spin state under pressure. We have also measured ZFC magnetization under pressure and obtained similar behavior of M and T_C [Supplementary information (Fig. S3)]. [36]

Mainly two competing magnetic interactions are responsible for determining the magnetic ground state of CrI_3 . The direct exchange between Cr-Cr is antiferromagnetic in nature. This direct exchange arises from the electron hopping between the nearest-neighbor Cr sites which is maximum when the Cr-Cr bond angle formed by $3d$ orbitals is 180° . On the other hand, depending on the symmetry relations and electron occupancy of the overlapping atomic orbitals, superexchange can be FM as well as antiferromagnetic (AFM) in nature and is mediated through a non-magnetic ligand ion. Unlike

the direct exchange, the superexchange interaction originates due to the virtual hopping of electrons between the two nearest-neighbor Cr ions via iodine ion. This virtual process reduces the total energy of the system. According to Goodenough-Kanamori-Anderson rules, when the magnetic-ion-ligand-magnetic-ion angle is 90° , the superexchange interaction is FM and is AFM, when the angle is 180° . [37–39]

In a weakly coupled layered van der Waals system, the effect of pressure on ferromagnetism is very sensitive to the bond angles and the inter-layer coupling. If the magnetic-ion-ligand-magnetic-ion bond angle is 90° then T_C is expected to decrease with application of external pressure because pressure may either increase or decrease the bond angle from 90° and as a result, the superexchange interaction which favors FM ordering may weaken. On the other hand, T_C may increase with pressure if the bond angle is lower or higher than 90° at ambient pressure. In such a situation, the bond angle may approach towards 90° with the application of pressure. It has already been mentioned that the effect of pressure on ferromagnetism investigated in bulk single crystal of $\text{Cr}_2\text{Ge}_2\text{Te}_6$ through magnetization measurements shows very different behavior from that we observe in CrI_3 . [32] In $\text{Cr}_2\text{Ge}_2\text{Te}_6$, T_C decreases monotonically with pressure up to about 9 % at 1 GPa. The pressure induced variations of magnetic properties in $\text{Cr}_2\text{Ge}_2\text{Te}_6$ has been attributed to lattice modulation arising due to strong spin-lattice coupling. The first-principles calculations show that the Cr-Cr bond length decreases while the Cr-Te-Cr bond angle gradually diverges from 90° with increasing pressure. Both these effects favor the direct exchange and weaken the superexchange interaction, i.e., AFM interaction in $\text{Cr}_2\text{Ge}_2\text{Te}_6$ enhances with pressure. Theoretical calculation also shows that the c/a ratio decreases with pressure. The reduction of c is relatively more significant than that of a due to the weak interlayer interaction and as a result, the interlayer coupling increases with pressure. As the interlayer van der Waals coupling in CrI_3 is weaker as compared to that in $\text{Cr}_2\text{Ge}_2\text{Te}_6$, the effect of pressure to increase the coupling between the two adjacent layers is significant in the former. In bulk CrI_3 , the interlayer coupling is FM in nature. Thus one expects that T_C will increase with the increase in pressure due to the enhancement of interlayer FM coupling. In VI_3 , another ferromagnet with weak van der Waals coupling, T_C increases with P above a threshold value of P , which has been attributed to crossover from two- to three-dimensionality due to the increase of interlayer coupling. [34] In order to understand, why CrI_3 exhibits highest T_C among the CrX_3 family and the effect of pressure on FM transition in CrI_3 is different from that in CrBr_3 , we first briefly discuss the evolution of magnetism in CrX_3 with the size of halogen ion X . As the Cr-Cr distance increases with increasing halogen size from Cl to Br to I, the direct exchange

weakens. Also, by moving from Cl to Br to I, the covalent nature of Cr-I bonds enhances which further strengthens superexchange interactions as well as the spin-orbit coupling and hence enhances the FM ordering temperature. [23] Recent experiments suggest that the covalent nature of Cr-I bond plays an important role in CrI_3 to have highest T_C among the CrX_3 family. [40]

In order to take into account the anisotropic nature of FM superexchange interaction via Cr-I-Cr, Lado and Fernandez-Rossier used anisotropic XXZ -type Hamiltonian with an additional term in the Heisenberg model, anisotropic symmetric exchange (λ), and estimated the Curie temperature from the spin wave theory. [23] They observe that T_C increases with the increase of λ . In fact, the nature of the variation of T_C with λ is very similar to that we observe from the pressure dependence. Another factor that may also play an important role to increase the T_C in CrI_3 system is the Cr-I-Cr bond angle. In CrI_3 , this bond angle is slightly larger than 90° . [23, 41] With increase in pressure, the Cr-I-Cr bond angle may approach towards 90° . We believe that the different role of pressure on the FM transition of CrI_3 and CrBr_3

is partly due to their structural anisotropy and partly due to the strong covalent nature of Cr-I-Cr bonding. High pressure structural analysis may reveal important information for understanding the role of pressure on FM interaction in CrX_3 series.

In conclusion, we have studied the magnetic properties of two-dimensional FM semiconductor CrI_3 with FM-PM phase transition temperature 60.4 K. Magnetization exhibits a clear anomaly below 212 K and a strong hysteresis between heating and cooling cycles, where a first-order structural transition is observed. Unlike the two-dimensional FM semiconductors CrBr_3 and $\text{Cr}_2\text{Ge}_2\text{Te}_6$, in the present system, T_C is found to increase monotonically from 60.4 to 64.9 K and the transition becomes sharper as the applied pressure increases from 0 to 1.0 GPa. The observed behavior suggests a strong spin-lattice coupling.

Acknowledgement: The authors acknowledge the technical support from A. Paul during sample preparation and the measurements. SA thanks DST (SERB, PURSE, FIST), UGC-DAE-CSR Indore, CEFIPRA, New Delhi. M.K thank CSIR for the fellowship.

-
- [1] K. S. Burch, D. Mandrus and J-G. Park, Nature (London) **563**, 47 (2018).
- [2] J-G. Park, J. Phys. Condens. Matter **28**, **301001** (2016)
- [3] B. Huang, G. Clark, D. R. Klein, D. MacNeill, E. Navarro-Moratalla, K. L. Seyler, N. Wilson, M. A. McGuire, D. H. Cobden, and D. Xiao et al., Nat. Nanotechnol. **13**, 544 (2018).
- [4] F. Hellman et al. Rev. Mod. Phys. **89**, 025006 (2017).
- [5] M. N. Baibich, J. M. Broto, A. Fert, F. Nguyen Van Dau, F. Petroff, P. Etienne, G. Creuzet, A. Friederich, and J. Chazelas, Phys. Rev. Lett. **61**, 2472 (1988).
- [6] G. Binasch, P. Grnberg, F. Saurenbach, and W. Zinn, Phys. Rev. B **39**, 4828 (1989).
- [7] M. Julliere, Phys. Lett. A. **54**, 225 (1975).
- [8] S. Datta and B. Das, Appl. Phys. Lett. **56**, 665 (1990).
- [9] D. Zhong, K. L. Seyler, X. Linpeng, R. Cheng, N. Sivadas, B. Huang et al., Sci. Adv. **3**, e1603113 (2017).
- [10] L. Onsager, Phys. Rev. **65**, 117 (1944).
- [11] N. D. Mermin and H. Wagner, Phys. Rev. Lett. **17**, 1133 (1966).
- [12] V. Berezinskii, Sov. Phys. JETP **32**, 493 (1971).
- [13] J. M. Kosterlitz and D. J. Thouless, J. Phys. C **6**, 1181 (1973).
- [14] R. Coldea, D. A. Tennant, E. M. Wheeler, E. Wawrzynska, D. Prabhakaran, M. Telling, K. Habicht, P. Smeibidl, and K. Kiefer, Science **327**, 177 (2010).
- [15] N. Sivadas, M. W. Daniels, R. H. Swendsen, S. Okamoto, and D. Xiao, Phys. Rev. B **91**, 235425 (2015).
- [16] M. A. McGuire, H. Dixit, V. R. Cooper, and B. C. Sales, Chem. Mater. **27**, 612 (2015).
- [17] C. Gong, L. Li, Z. L. Li, H. W. Ji, A. Stern, Y. Xia, T. Cao, W. Bao, C. Z. Wang, Y. Wang, Z. Q. Qiu, R. J. Cava, S. G. Louie, J. Xia, and X. Zhang, Nature (London) **546**, 265 (2017).
- [18] B. Huang, G. Clark, E. Navarro-Moratalla, D. R. Klein, R. Cheng, K. L. Seyler, D. Zhong, E. Schmidgall, M. A. McGuire, D. H. Cobden, W. Yao, D. Xiao, P. Jarillo-Herrero, and X. D. Xu, Nature (London) **546**, 270 (2017).
- [19] Y. Liu and C. Petrovic, Phys. Rev. B **97**, 014420 (2018).
- [20] M. A. McGuire, G. Clark, S. KC, W. M. Chance, G. E. Jellison, Jr., V. R. Cooper, X. D. Xu, and B. C. Sales, Phys. Rev. Mater. **1**, 014001 (2017).
- [21] Z. Wang, I. Gutiérrez-Lezama, N. Ubrig, M. Kroner, T. Taniguchi, K. Watanabe, A. Imamoğlu, E. Giannini, and A. F. Morpurgo, Nature Commun. **9**, 2516 (2018).
- [22] L. Webster and J-A. Yan, Phys. Rev. B **98**, 144411 (2018).
- [23] J. L. Lado and J. F. Rossier, 2D Mater. **4**, 035002 (2017).
- [24] M. Sakashita, H. Yamawaki, H. Fujihisa, K. Aoki, S. Sasaki, and H. Shimizu, Phys. Rev. Lett. **79**, 1082 (1997).
- [25] M. P. Pasternak, G. Kh. Rozenberg, G. Yu. Machavariani, O. Naaman, R. D. Taylor, and R. Jeanloz, Phys. Rev. Lett. **82**, 4663 (1999).
- [26] L. Forró, R. Gaál, H. Berger, P. Fazekas, K. Penc, I. Kézsmrki, and G. Mihály, Phys. Rev. Lett. **85**, 1938 (2000).
- [27] A. P. Drozdov, M. I. Eremets, I. A. Troyan, V. Ksenofontov and S. I. Shylin, Nature (London) **525**, 73 (2015).
- [28] P. Sarkar, P. Mandal, K. Mydeen, A. K. Bera, S. M. Yusuf, S. Arumugam, C. Q. Jin, T. Ishida, and S. Noguchi, Phys. Rev. B **79**, 144431 (2009).
- [29] P. Sarkar, S. Arumugam, P. Mandal, A. Murugeswari, R. Thiagarajan, S. E. Muthu, D. M. Radheep, C. Ganguli, K. Matsubayshi, and Y. Uwatoko, Phys. Rev. Lett. **103**, 057205 (2009).
- [30] L. Demkó, I. Kézsmárki, G. Mihály, N. Takeshita, Y.

- Tomioka, and Y. Tokura, Phys. Rev. Lett. **101**, 037206 (2008).
- [31] T. Kanomata, T. Tsuda, H. Yasui and T. Kaneko, Phys. Lett. A **134**, 196 (1988).
- [32] Y. Sun, R. C. Xiao, G. T. Lin, R. R. Zhang, L. S. Ling, Z. W. Ma, X. Luo, W. J. Lu, Y. P. Sun, and Z. G. Sheng, Appl. Phys. Lett. **112**, 072409 (2018).
- [33] H. Yoshida, J. Chiba, T. Kaneko, Y. Fujimori, and S. Abe, Physica B **237-238**, 525 (1997).
- [34] S. Son, Matthew J. Coak, N. Lee, J. Kim, T. Y. Kim, H. Hamidov, H. Cho, C. Liu, D. M. Jarvis, P. A. C. Brown, J. H. Kim, C.-H. Park, D. I. Khomskii, S. S. Saxena, and J.-G. Park, arXiv:1812.05284.
- [35] Y. Liu and C. Petrovic, Phys. Rev. B **97**, 174418 (2018).
- [36] See Supplemental Material (link will be provided by the publisher) for effect of hydrostatic pressure on ferromagnetism in two-dimensional CrI₃.
- [37] P. W. Anderson, Phys. Rev. **79**, 350 (1950).
- [38] J. B. Goodenough, Phys. Rev. **100**, 564 (1955).
- [39] J. Kanamori, J. Phys. Chem. Solids **10**, 87 (1959).
- [40] A. Frisk, L. B. Duffy, S. Zhang, G. van der Laan, and T. Hesjedal, Materials Lett. **232**, 5 (2018).
- [41] S. Feldkemper and W. Weber, Phys. Rev. B **57**, 7755 (1998).